

Numerical Kinematic Analysis of the Standard Macpherson Motor-Vehicle Suspension System

Hazem Ali Attia*

*Department of Mathematics, College of Science, King Saud University,
(Al-Qasseem Branch), P.O.Box 237, Buraidah 81999, KSA*

In this paper, an efficient numerical algorithm for the kinematic analysis of the standard MacPherson suspension system is presented. The kinematic analysis of the suspension mechanism is carried out in terms of the rectangular Cartesian coordinates of some defined points in the links and at the kinematic joints. Geometric constraints that fix the distances between the points belonging to the same rigid link are introduced. The nonlinear constraint equations are solved by iterative numerical methods. The corresponding linear equations of the velocity and acceleration are solved to yield the velocities and accelerations of the unknown points. The velocities and accelerations of other points of interest as well as the angular velocity and acceleration of any link in the mechanism can be calculated.

Key Words : Kinematic Analysis, Mechanisms and Machines, Suspension Systems, Position Problem, Velocity and Acceleration Problems

1. Introduction

The different analytical methods for kinematic analysis of mechanisms can be classified according to the type of coordinates chosen to formulate their constraints and determine their configuration. Some formulations use a large set of absolute coordinates (Wehage and Haug, 1982; Nikravesh, 1988). The position and orientation of the rigid links in the mechanism are described with respect to the global reference coordinate system. The algebraic equations of constraints are introduced to represent the kinematic joints that connect the rigid bodies. Although in this type of formulation the constraint equations are easy to construct, it has the disadvantage of the large number of defined dependent coordinates.

Other formulations use sets of relative coordi-

nates (Denavit and Hartenberg, 1955; Paul and Krajcinovic, 1970). The position of each link is defined with respect to the previous link by means of relative joint coordinates that depend on the type of the joint connecting the two links. This type of formulation yields a minimal set of algebraic equations. The constraint equations are derived based on loop closure equations, and the resulting constraint equations are highly nonlinear and contain complex sinusoidal functions.

Another formulation which is based on point coordinates is discussed in (Garcia de Jalon et al., 1981, 1982; Vilallonga et al., 1984; Akhras and Angeles, 1990; Attia, 1993, 1999; Attia and Amasha, 2001). The configuration of the system is described in terms of the rectangular Cartesian coordinates of some defined points in the links and at the joints. The system constraint equations are then written to fix the relative positions of the points in each rigid link and also the relative positions between the different links determined by the type of joints connecting them.

In this paper the kinematic analysis of the standard MacPherson suspension system is carried out in terms of point coordinates. The posi-

* E-mail : ah1113@yahoo.com

TEL : +966-6-3800319; FAX : +966-6-3800911-9312
Department of Mathematics, College of Science, King Saud University, (Al-Qasseem Branch), P.O.Box 237, Buraidah 81999, KSA. (Manuscript Received May 10, 2003; Revised September 16, 2003)

tion, velocity, and acceleration analyses are carried out to determine the positions, velocities, and accelerations of the unknown points and links in the mechanism. The velocities and accelerations of other points of interest can also be calculated if their positions are locally specified. The angular velocity and acceleration of any link in the mechanism are evaluated in terms of the Cartesian coordinates, velocities, and accelerations of the assigned points. The presented formulation in terms of the Cartesian coordinates of specified link points is simple and involves only elementary mathematics.

2. Modelling of the Standard Macpherson Suspension

Figure 1 presents a schematic diagram of a quarter of a car with the standard MacPherson suspension system that has different kinematic joints. The mechanical system consists of the main chassis, a standard MacPherson suspension mechanism, a steering rod and a wheel. The standard MacPherson suspension consists of an A-arm, a knuckle and a spring rod. The system constitutes two closed loops. The first closed loop is composed of the chassis, the A-arm, the knuckle and the steering rod. The second closed loop is composed of the chassis, the A-arm, the knuckle and the spring rod. The chassis is constrained to move vertically upward or downward. The steering rod connects the chassis and the knuckle via two spherical joints and it represents a kinematic constraint imposed on the system. The A-arm and the knuckle each has 6 degrees of freedom and the spring rod has 5 degrees of freedom (no rotation about its axis) in spatial motion. One revolute joint connects the chassis and the A-arm and imposes 5 constraints. Two spherical joints each imposes 3 constraints: one connects the A-arm to the knuckle and the other connects the chassis and the spring rod. One translational joint connects the spring rod to the knuckle and imposes 5 constraints. Thus the system has 2 degrees of freedom.

The configuration of the mechanism can be specified by defining a set of points on the links

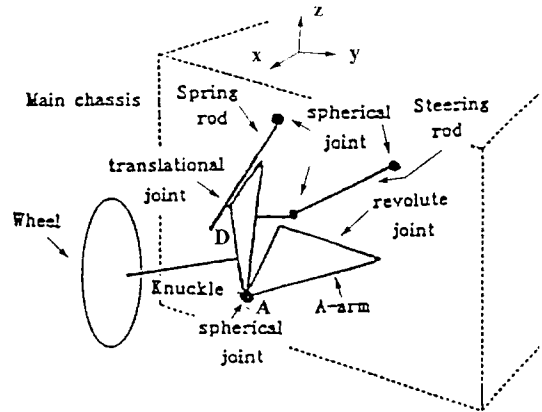


Fig. 1 Schematic Diagram of the MacPherson suspension indicating the kinematic joints

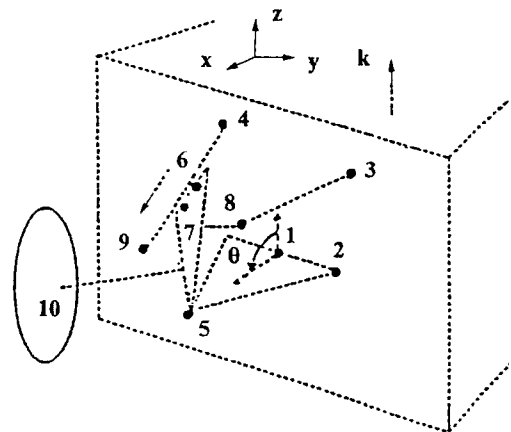


Fig. 2 Schematic Diagram of the MacPherson suspension with the assigned points

and joints. Figure 2 presents the standard MacPherson mechanism with its assigned points. Each binary link is replaced by two points located at both ends while each ternary link is replaced by three points. The adjacent links share common points. Two points are located at the axis of the revolute joint connecting the chassis and the A-arm to define its direction (points 1 and 2). Points 3 and 4 are located at the centers of the spherical joints connecting the chassis to the steering and the spring rods respectively. Points 5 and 8 are located at the centers of the spherical joints connecting the knuckle to the A-arm and the steering rod respectively. The locations of these points (points 1, ..., 5 and 8) are chosen to

automatically eliminate the constraint equations associated with the revolute and spherical joints. Points 6, 7 and 9 together with point 4 are located along the axis of the translational joint to define its orientation and to help in constructing the vectors needed to write the constraint equations associated with this kinematic joint. The initial positions, velocities and accelerations of points 1, ..., 4 are known from the input data of the driver. Points 5, ..., 9 are the unknown points and their Cartesian coordinates define the motion variables. Therefore, 15 constraint equations are needed to solve for the 15 unknown Cartesian coordinates. Having determined the configuration of the mechanism in terms of the unknown points, the location of any other point of interest can also be calculated.

2.1 Position analysis

The constraints are either geometric or kinematic constraints. The geometric constraints are distance constraints between pairs of points belonging to the same link. For the steering rod of fixed length, a distance constraint that fixes the distance between points 3 and 8 is written. For a ternary link, three distance constraints are written to fix the distance between each pair of the three points replacing the link. The geometric constraint equations are expressed in the Cartesian coordinates of the points as follows,

$$(x_5 - x_1)^2 + (y_5 - y_1)^2 + (z_5 - z_1)^2 - d_{5,1}^2 = 0 \quad (1)$$

$$(x_5 - x_2)^2 + (y_5 - y_2)^2 + (z_5 - z_2)^2 - d_{5,2}^2 = 0 \quad (2)$$

$$(x_8 - x_3)^2 + (y_8 - y_3)^2 + (z_8 - z_3)^2 - d_{8,3}^2 = 0 \quad (3)$$

$$(x_9 - x_4)^2 + (y_9 - y_4)^2 + (z_9 - z_4)^2 - d_{9,4}^2 = 0 \quad (4)$$

$$(x_6 - x_5)^2 + (y_6 - y_5)^2 + (z_6 - z_5)^2 - d_{6,5}^2 = 0 \quad (5)$$

$$(x_7 - x_5)^2 + (y_7 - y_5)^2 + (z_7 - z_5)^2 - d_{7,5}^2 = 0 \quad (6)$$

$$(x_8 - x_5)^2 + (y_8 - y_5)^2 + (z_8 - z_5)^2 - d_{8,5}^2 = 0 \quad (7)$$

$$(x_7 - x_6)^2 + (y_7 - y_6)^2 + (z_7 - z_6)^2 - d_{7,6}^2 = 0 \quad (8)$$

$$(x_8 - x_6)^2 + (y_8 - y_6)^2 + (z_8 - z_6)^2 - d_{8,6}^2 = 0 \quad (9)$$

$$(x_8 - x_7)^2 + (y_8 - y_7)^2 + (z_8 - z_7)^2 - d_{8,7}^2 = 0 \quad (10)$$

where $d_{i,j}$ is the distance between points i and j

belonging to the same rigid link and $x_i, y_i,$ and z_i are the Cartesian coordinates of point i , respectively. Kinematic constraints result from the conditions imposed by the kinematic joints on the relative motion between the bodies they comprise. Points located at the centre of a spherical joint or the axis of a revolute joint automatically eliminates all the kinematic constraints due to these joints. However, because of the presence of the translational joint, kinematic constraints are added in terms of the coordinates of the points located along the axis of the translational joint. Two points on each body are located along the axis of the joint and the constraint formulation should ensure that the four points remain colinear. The independent kinematic constraints resulting from the cross product operation take the form,

$$(y_7 - y_6)(z_9 - z_4) - (z_7 - z_6)(y_9 - y_4) = 0 \quad (11)$$

$$(x_7 - x_6)(z_9 - z_4) - (z_7 - z_6)(x_9 - x_4) = 0 \quad (12)$$

$$(y_9 - y_7)(z_9 - z_4) - (z_9 - z_7)(y_9 - y_4) = 0 \quad (13)$$

$$(x_9 - x_7)(z_9 - z_4) - (z_9 - z_6)(x_9 - x_4) = 0 \quad (14)$$

Equations (11) and (12) ensure that the two bodies remain parallel to each other. However, Eqs. (13) and (14) are sufficient to prevent the separation between the two bodies. Moreover, a driving constraint is added to the above constraints as a function of the input driving variable, namely, the angular coordinate θ (see Fig. 2) in the form,

$$(z_5 - z_1) - d_{5,1} \cos(\theta) = 0 \quad (15)$$

where θ is the inclination angle of the line connecting points 1 and 5 with the vertical upwards.

Eq. (1) expresses the required 15 independent constraint equations in terms of the Cartesian coordinates of the assigned points. The vector of coordinates composes known and unknown sets of coordinates. The known coordinates are the coordinates of points 1, 2, 3 and 4 fixed on the chassis, and the driving coordinate θ . They should be given at any instant. The unknown coordinates are the 15 Cartesian coordinates of points 5, 6, 7, 8 and 9 located on the knuckle

and the spring rod. Given the set of known coordinates at each instant of time, the 15 non-linear Eq. (1) can be solved by any iterative numerical method (Molian, 1968) to determine the 15 unknown Cartesian coordinates.

It should be noted that in this formulation, the kinematic constraints due to some common types of kinematic joints (e.g. revolute or spherical joints) can be automatically eliminated by properly locating the assigned points. The remaining kinematic constraints along with the geometric constraints are, in general, either linear or quadratic in the Cartesian coordinates of the particles. Therefore, the coefficients of their Jacobian matrix are constants or linear in the rectangular Cartesian coordinates. Whereas in the formulation based on the relative coordinates, the constraint equations are derived based on loop closure equations which have the disadvantage that they do not directly determine the positions of the links and points of interest which makes the establishment of the dynamic problem more difficult. Also, the resulting constraint equations are highly nonlinear and contain complex circular functions. The absence of these circular functions in the point coordinate formulation leads to faster convergence and better accuracy. Furthermore, preprocessing the mechanism by the topological graph theory is not necessary as it would be the case with loop constraints.

Also, in comparison with the absolute coordinates formulation, the manual work of the local axes attachment and local coordinates evaluation as well as the use of the rotational variables and the rotation matrices in the absolute coordinate formulation are not required in the point coordinate formulation. This leads to fully computerized analysis and accounts for a reduction in the computational time and memory storage. In addition to that, the constraint equations take much simpler forms as compared with the absolute coordinates.

The main kinematical properties of the suspension are described by the coordinates of the wheel centre point and the kingpin angle α and camber angle β (Adler, 0000). The wheel centre point (point 10, see Fig. 2) is defined as the point at

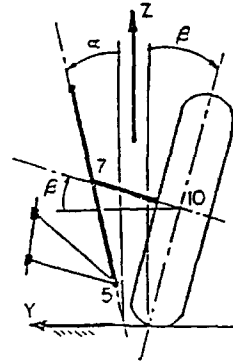


Fig. 3 Kingpin and camber angles

which the wheel spin axis intersects the wheel plane. Points 7 and 10 define the wheel spin axis. The coordinates of the wheel centre point can be determined by specifying its position relative to three other points 5, 6, and 7 on the knuckle. Then, three distance constraints can be solved iteratively to get its global coordinates. Kingpin angle determines the steering aligning torque in conjunction with steering offset and wheel caster. The kingpin angle α is defined as the inclination angle of the steering axis AD relative to the vertical longitudinal plane, measured in the transverse plane of the vehicle (Adler, 0000) and therefore from Fig. 3;

$$\alpha = \tan^{-1}[(y_7 - y_5) / (z_7 - z_5)] \quad (16)$$

A positive angle α signifies a displacement of point 5 in the negative y direction. The camber angle β is the inclination of the wheel plane relative to the longitudinal vehicle plane, measured in the transverse plane of the vehicle and therefore;

$$\beta = \tan^{-1}[-(z_7 - z_{10}) / (y_7 - y_{10})] \quad (17)$$

Positive camber means that the wheels are tilted out at the top than at the bottom.

2.2 Velocity and acceleration analyses

The velocity equations are derived by differentiating Eq. (1) with respect to time. Then:

$$[C_q] \dot{\mathbf{q}} = 0 \quad (18)$$

where the constraint Jacobian matrix $[C_q]$ contains partial derivatives of the constraint equations with respect to the coordinates of the points.

known points can be determined by solving the linear Eqs. (19) and (23) respectively using any numerical method. The velocities and accelerations of any other points of interest can be calculated. Also the angular velocity and acceleration of any link in the mechanism can be evaluated from the Cartesian coordinates, velocities, and accelerations of any three defined points on the link. The vectors of the angular velocity and acceleration of the ternary link can be determined as follows,

$$\omega = \frac{\mathbf{v}_{7,6} \times \mathbf{v}_{8,6}}{\mathbf{v}_{7,6} \cdot \mathbf{r}_{8,6}}, \quad \alpha = \frac{\hat{\mathbf{a}}_{7,6} \times \hat{\mathbf{a}}_{8,6}}{\hat{\mathbf{a}}_{7,6} \cdot \mathbf{r}_{\pi,6}} \quad (25)$$

where $\hat{\mathbf{a}}_{j,i} = \mathbf{a}_{j,i} - \omega \times (\omega \times \mathbf{r}_{j,i})$ and i, j , and k are the indices of three points located on the rigid link. Vectors $\mathbf{r}_{j,i}$, $\mathbf{v}_{j,i}$, and $\mathbf{a}_{j,i}$ are the relative position, velocity, and acceleration vectors between points j and i , respectively.

3. Results of the Simulation

The chassis is assumed to be stationary and therefore the values of the velocities and acc-

elerations of all known points (points 1, ..., 4) fixed on it are identically zero. The Cartesian coordinates of the known points are listed in Table 1. The driving variable θ is taken as function of time in the form, $\theta(t) = 1 + t + t^2$. The nonlinear equations of constraints (1) are solved by Newton-Raphson's method of successive approximation to determine the Cartesian coordinates of the unknown points for different time steps. Also, the Cartesian coordinates of the wheel centre (point 10) are estimated. The velocity and acceleration equations are solved using the L-U factorization with pivoting method. Table 2 presents some results of the kinematic analysis for two seconds of simulation as a result of changing the driver angle with time. The positions, velocities and accelerations of some points in the mechanism are indicated. The angular velocity and angular acceleration of the knuckle are also shown at various time levels. Figure 4 presents the time variation of the z-coordinate of the wheel centre. Figure 5 shows the variation of the kingpin angle α and the camber angle β with time.

Table 1 Cartesian coordinates (m) of the known points

(x_1, y_1, z_1)	(1.495, 0.05, -0.08)	(x_3, y_3, z_3)	(1.11, -0.02, 0.06)
(x_2, y_2, z_2)	(1.175, 0.05, -0.08)	(x_4, y_4, z_4)	(1.38, 0.28, 0.49)

Table 2 Simulation Results
Time (s), x (m), \dot{x} (m/s), \ddot{x} (m/s²), ω (rad/s), α (rad/s²)

Time	0	1	2
(x_8, y_8, z_8)	(1.29, 0.39, 0.2)	(1.3, 0.27, -0.26)	(1.295, 0.4, 0.1)
$(\dot{x}_8, \dot{y}_8, \dot{z}_8)$	(0, 0.09, -0.26)	(0.01, -0.48, -0.4)	(-0.02, -0.13, 1)
$(\ddot{x}_8, \ddot{y}_8, \ddot{z}_8)$	(0.04, 0.0, -0.6)	(-0.02, -0.49, 0.8)	(0.026, -2.2, -1)
(x_9, y_9, z_9)	(1.5, 0.4, 0.13)	(1.4, 0.3, 0.09)	(1.48, 0.41, 0.13)
$(\dot{x}_9, \dot{y}_9, \dot{z}_9)$	(-0.13, 0.1, -0.01)	(-0.02, -0.3, -0.02)	(0.26, 0.22, 0.08)
$(\ddot{x}_9, \ddot{y}_9, \ddot{z}_9)$	(0.04, -0.4, -0.06)	(0.135, -0.257, 0.2)	(1.2, -2.5, -0.4)
(x_{10}, y_{10}, z_{10})	(1.6, 0.39, 0.05)	(1.58, 0.34, -0.469)	(1.59, 0.5, -0.05)
$(\dot{x}_{10}, \dot{y}_{10}, \dot{z}_{10})$	(-0.03, 0.26, -0.3)	(-0.007, -0.6, -0.5)	(0.077, -0.4, 1)
$(\ddot{x}_{10}, \ddot{y}_{10}, \ddot{z}_{10})$	(-0.01, -0.2, -0.5)	(0.14, -1.49, 0.82)	(0.19, -4.0, -0.6)
$\omega_{knuckle}$	(0.11, 0.2, 0.47)	(-0.68, 0.07, -0.16)	(0.37, -0.3, -1.1)
$\alpha_{knuckle}$	(-1, -0.2, -0.12)	(-0.17, 0.3, -3.4)	(-5.3, -2.3, -2.6)

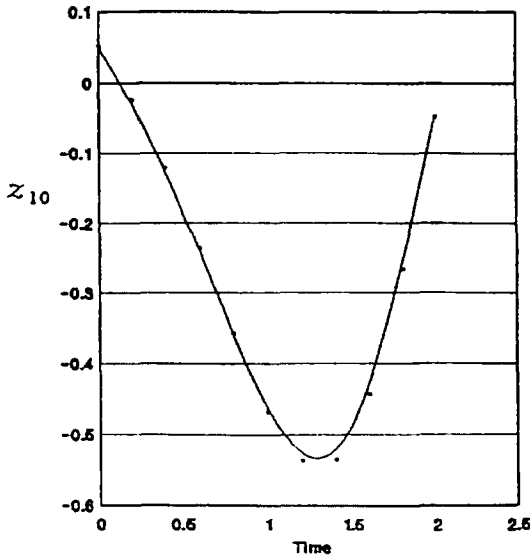


Fig. 4 Time (s) variation of z_{10} (m)

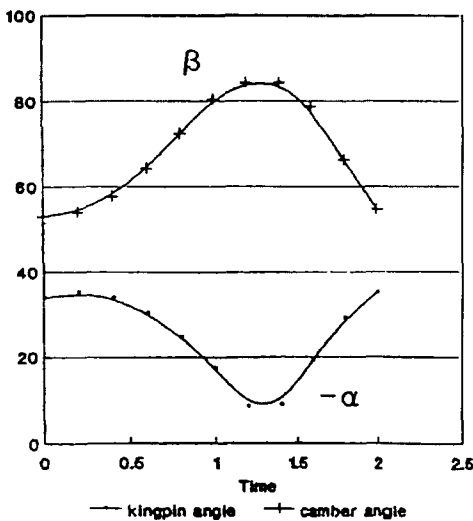


Fig. 5 Time (s) variation of the kingpin and camber angles (Deg)

4. Conclusions

In this paper, the numerical kinematic analysis of the standard MacPherson suspension system is presented. The kinematic analysis is carried out in terms of the rectangular Cartesian coordinates of some defined points in the links and at the kinematic joints. The suggested algorithm eliminates the need to write redundant constraints

and allows solving a reduced system of equations. This reduced system of equations results in a better accuracy and a reduction in computing time and memory storage in comparison with the absolute coordinate formulation. The algorithm can be used to solve for the initial position as well as the finite displacement problems. The results of the analysis indicate the simplicity, generality, and efficiency of the proposed algorithm.

References

Adler, U., *Automotive Handbook*, Bosch, FDI-Verlag, Approved Edition Under Licence SAE, ISPN 089283-518-6.

Akhras, R. and Angeles, J., 1990, "Unconstrained Nonlinear Least-Square Optimization of Planar Linkages for Rigid-Body Guidance," *Mechanism and Machine Theory*, Vol. 25, pp. 97~118.

Attia, H. A. and Amasha, H. M., 2001, "An Efficient Algorithm for the Kinematic Analysis of Planar Mechanisms," *Proceedings of the Eighth IFToMM International Symposium on Theory of Machines and Mechanisms (SYROM 2001)*, ARoTMM Bucharest, Romania, Vol. I, pp. 31~36, Aug. 28-Sept. 1.

Attia, H. A., 1993, *A Computer-Oriented Dynamical Formulation with Applications to Multi-body Systems*. Ph. D. Dissertation, Department of Engineering Mathematics and Physics, Faculty of Engineering, Cairo University.

Attia, H. A., 1999, "A Numerical Method for the Kinematic Analysis of Spatial Mechanisms," *CSME Transactions*, Vol. 23, No. 1A, pp. 71~82.

Denavit, J. and Hartenberg, R. S., 1955, "A Kinematic Notation for Lower-Pair Mechanisms Based on Matrices," *ASME Journal of Applied Mechanics*, pp. 215~221.

Garcia de Jalon, J., Serna, M. A. and Aviles, R., 1981, "Computer Method for Kinematic Analysis of Lower-Pair Mechanisms-I Velocities and Accelerations," *Mechanism and Machine Theory*, Vol. 16, pp. 543~556.

Garcia de Jalon, J., Serna, M. A. and Aviles, R., 1981, "Computer Method for Kinematic

Analysis of Lower-Pair Mechanisms-II Position Problems," *Mechanism and Machine Theory*, Vol. 16, pp. 557~566.

Garcia de Jalon, J. et al., 1982, "Simple Numerical Method for the Kinematic Analysis of Spatial Mechanisms," *ASME Journal on Mechanical Design*, Vol. 104, pp. 78~82.

Molian, S., 1968, "Solution of Kinematics Equations by Newton's Method," *Journal of Mechanical Engineering Science*, Vol. 10, No. 4, pp. 360~362.

Nikravesh, P. E., 1988, *Computer-Aided Analysis of Mechanical Systems*, Prentice-Hall.

Paul, B. and Krajcinovic, D., 1970, "Computer

Analysis of Machines with Planar Motion-1. Kinematics, 2. Dynamics," *ASME Journal of Applied Mechanics*, Vol. 37, pp. 697~712.

Vilallonga, G., Unda, J. and Garcia de Jalon, J., 1984, "Numerical Kinematic Analysis of Three-Dimensional Mechanisms Using a 'Natural' System of Lagrangian Coordinates," *ASME Paper No. 84-DET-199*.

Wehage, R. A. and Haug, E. J., 1982, "Generalized Coordinate Partitioning of Dimension Reduction, in Analysis of Constrained Dynamic Systems," *ASME Journal of Applied Mechanical Design*, Vol. 104, pp. 247~255.